Faculty of Pharmacy[1], Phamacologic and Diagnostic Research Center (PDRC), Al-Ahliyya Amman University; Faculty of Pharmacy and Medical Sciences[2], University of Petra; Faculty of Pharmacy[3], University of Jordan, Amman, Jordan

# Synthesis and characterization of mesoporous silica and its application as drug delivery system for glimepiride

F. Muhana[1], I. Al-Ani[1], F. Al-Akayleh[2], D. Marzouqa[3], F. Khalili[3], H. Al-Khatib[2], H. Mutti[1], N. Shalan[1]

*Received January 7, 2021, accepted February 13, 2021*

**Corresponding author: Dr. Frezah Muhana Faculty of Pharmacy, Phamacologic and Diagnostic Research Center (PDRC), Al-Ahliyya Amman University, PO Box: 108, Amman, Jordan*
*F.muhana@ammanu.edu.jo, Fhmuhana@gmail.com*

*Pharmazie 76: 300-307 (2021)* *doi: 10.1691/ph.2021.1309*

The objective of this study was to synthesize the mesoporous silicate SBA-15 loaded with glimeperide, a slightly soluble antidiabetic, and to investigate the impact of drug loading on the release of glimepiride from this carrier. SBA-15 mesospheres were synthesized by addition of HCl to the trico-polymer (PEO20PPO70PEO20) until complete dissolution, then by addition of tetraethyl orthosilicate, stirring and drying until mesospheres powder was received. The mesopheres were characterized by thermal gravimetric analysis, powder X-ray diffraction, and Fourier transfer infrared analysis. The morphology was examined under a Scanning Electron Microscope. The surface area of the prepared mesospheres was determined by Brunauer-Emmett-Teller and the compression behavior of the powder was also studied. Then glimepiride was loaded on the mesospheres and percent loading as well as drug release was studied. Results showed successful preparation of the mesospheres with a glimepiride loading of was 40% with significant release improvement of glimepiride dissolution. A proportion of 70% glimepiride was released in the first 10 min compared to 5 % pure drug. It was concluded that the prepared mesospheres highly improve dissolution of glimeperide.

## 1. Introduction

Inorganic mesoporous silicates materials are a promising class of synthetic polymers, widely used in catalysis reactions (Malhis et al. 2018), drug delivery and adsorbents for toxicants. Mesoporous silicate materials have many attractive physicochemical characteristics, such as large surface and pore volume which permits the binding of a different functional group for targeted the drug entity, with tunable pore sizes. They have an open framework pore structure (Abdelhamid 2000), thermal and chemical stability, are cheap, safe, hydrophilic and easily synthesizable. They have enriched surface silanol groups and a modifiable surface (Zhao et al. 2017) to expand their scope of application. In addition, many studies have shown that mesoporous silica materials have good biocompatibility and biodegradability in animal and plant cells (Fruijtier-Pölloth 2012).

The family of ordered mesoporous materials known as SBA (Santa Barbra Amorphous Material) was first synthesized in 1995. It was prepared using templates based on block copolymers (Zhao et al. 1998). A member of this family is the 2-D hexagonal mesoporous material coded SBA-15.

This material exhibits highly ordered hexagonal cylinders with main characteristics (depending on the synthesis conditions), a pore diameter in the range 4.6-30 nm and surface area of 690-1040 $m^2/g$ (da Silva et al. 2010).

SBA-15 is easily prepared by sol-gel synthesis, the mechanism of synthesis involves cooperative self-assembly of the inorganic molecular species (Abbaspour et al. 2012). In acidic solution, the hydrophilic ethylene oxide moieties are expected to interact with the protonated silanol groups, and thus will be closely associated with the inorganic walls. Increasing the temperature results in an increase in the hydrophobicity of ethylene oxide segments that are associated with the silica wall. This tends to increase the hydrophobic volume of the surfactant aggregates, resulting in increased pore size in SBA-15 material that is prepared at 80 °C (Zhao et al. 1998). SBA-15 has been utilized as a support material in heterogeneous catalyzes (Ziarani et al. 2011), as a sorbent for heavy metal ions, in advanced optical materials (Liu et al. 2000), a selective sorbent for proteins (Han et al. 1999) as a template for nano-wires (Huang et al. 2000), and has recently been employed in drug delivery systems (DDS) (Vallet-Regi et al. 2001).

SBA-15 was first employed as a DDS for gentamicin as a model drug (Doadrio et al. 2004). Since then, it was also used as a drug delivery system for several drugs such as ibuprofen (Izquierdo-barba et al. 2009), , amoxicillin (Izquiredo-barba et al. 2004), captopril (Qu et al. 2006), alendronate (Balas et al. 2006; Vallet-Regi et al. 2007), erythromycin (Doadrio et al. 2006), atenolol (Fagundes et al. 2006), itraconazole (Mellaert et al. 2008), salicylic acid (Rosenholm et al 2008), nimodipine (Yu et al. 2009), vancomycin (Doadrio et al. 2010), and etravirine (Mellaert et al. 2013).

Glimepiride is a third generation sulfonylurea (Massi-Benedetti 2003) with a molecular formula of C24H34N4O5S (Tiwari et al. 2016) and a molecular mass of about 490.617g/mol that has been introduced in 1995 to treat type –II diabetes mellitus (Rani et al. 2014). Glimepiride is a highly hydrophobic drug and it is insoluble both in water and acidic media, hence it is classified as a BCS (Biopharmaceutical Classification System) class-II drug (Chaudhari et al. 2012). The delivery of glimepiride in an active and absorbable form to the desired absorption site using physiologically safe excipients is very challenging (Amidon et al. 1995). In addition, this drug is slightly soluble in many buffers and organic solvents like methylene chloride (dichloromethane), very slightly soluble in methanol while soluble in dimethyl sulfoxide (DMSO) (Bala et al. 2014). Glimepiride shows low pH dependent solubility, i.e., glimepiride exhibits very poor solubility at 37 °C (<0.004 mg/ml) in acidic and neutral aqueous media while in pH>7, glimepiride solubility can reach 0.02 mg/ml (Wagh et al. 2012).

The objective of this paper was to synthesize the mesoporous silicate SBA-15 and to investigate the impact of drug loading on the release of glimepiride from this carrier, aiming to improve drug

solubility and control drug release. Thermal profiles, FTIR spectra, BET study, particle morphology and the compression profile using Heckel and Kawakita were also studied to confirm the nature of the drug within the carrier system and the presence or lack of surface crystals. These studies will elucidate the loading efficiency, release behavior, and the nature of the drug within mesoporous carriers.

## 2. Investigations, results and discussion

### *2.1. Synthesis of mesoporous carrier SBA-15*

Mesoporous silicates SBA-15 particulates were prepared using the self-assembly method. A typical synthesis of SBA-15 requires a minimum of four reagents: a solvent, a silica precursor, an ionic (anionic or cationic), or a non-charged surfactant and a catalyst. Depending on the protocol, the reaction could occur in an acidic or basic medium, with different silica/surfactant ratios (Bhattacharyya et al. 2006). In this study, the synthesis was done in alkaline media using TEOS as silica source, triblock copolymer (PEO20PPO70PEO20) as structure-directing agent, and water to decrease the hydrolysis rate of TEOS. Calcination was used as the method for removing the surfactant. It is the most common way to completely remove the surfactants in a way that is as cheap and time effective as possible.

### *2.2. Glimepiride loading into SBA-15*

There are various factors that influence the drug loading into mesoporous silica, such as the type of solvent, loading process, accessible surface area, and the pore volume of the mesoporous silica. Solvent-based method was used to load the glimepiride into the mesoporous silicate SBA-15. It was conducted using ethanol with different portions, to optimize the maximum loading of drug in the carrier. Although the solvent-free method has a lower environmental impact with no need for checking the residual solvent in the final product, the solvent-based method is a more practical and straightforward solution for drug amorphization within mesoporous silica. In general, solvent-based loading techniques produce drug-loaded mesoporous silica with a high loading efficiency compared to solvent-free techniques (Le et al. 2019). Different ratios of ethanol solution were used as the loading solvent to enhance drug solubility and to maximize the loading efficiency.

$$\%\ Drug\ Loading = \frac{2006\mu g}{5000\mu g} \times 100\% = 40.12\%$$

### *2.3. Characterization of the mesoporous carrier SBA-15*

#### *2.3.1. Thermal gravimetric analysis (TGA)*

The Thermal Gravimetric Analysis of SBA-15 (Fig. 1) showed two main stages of weight loss. The first stage represents desorption of the water molecules that are hydrogen-bonded to the surface silanol groups and water bulk molecules occupying within the pores, it takes place around 25-200 °C. The second stage of the weight loss is attributed to the thermal dehydration of surface silonol groups at approximately (300-1000 °C) (Schumacher et al. 1999)
Drug loading was confirmed by TGA. The TGA curves in Fig. 1 show that glimepiride is thermally stable up to about 198 °C and then decomposes in the first stage up to 269.31 °C with a mass loss of 31.75% which suggests the loss of $C_8H_{15}N_2O$ fragment (Attia et al. 2013). Glimepiride continues to decompose from 269.31 °C to 369 °C in the second stage of decomposition showing a mass loss of 39.66% due to the loss of $C_{10}H_{15}N_2O_2$ part and the third and last stage in the temperature range of 369-690 °C (56.23%) is due to the loss of $C_6H_4SO_2$.

#### *2.3.2. Powder X- ray diffraction (PXRD)*

The diffraction spectrum of pure glimepiride showed that the drug was of crystalline nature as demonstrated by nemours peaks. Numerous diffraction peaks of glimepiride were observed at 2θ of 13.41, 14.62, 16.67, 18.13, 19.18, 21.03, 21.11, 22.95 and 26.33 (Fig. 2) indicating crystalline glimepiride (Singh et al. 2009). Pure SBA-15 showed three reflections, at 2θ values, this includes a strong peak at 1.2 and two weak peaks and at 1.9 and 2.2 respectively. This corresponds to a highly ordered hexagonal mesoporous silica framework (Zhao et al.1998) and a two dimensional (2D) hexagonal mesostructured with space group p6mm. All principal peaks from SBA-15 and glimepiride were present in XRD pattern drug loaded carrier although with lower intensity, but no new peaks could be observed suggesting the absence of chemical interaction between the drug and carrier.

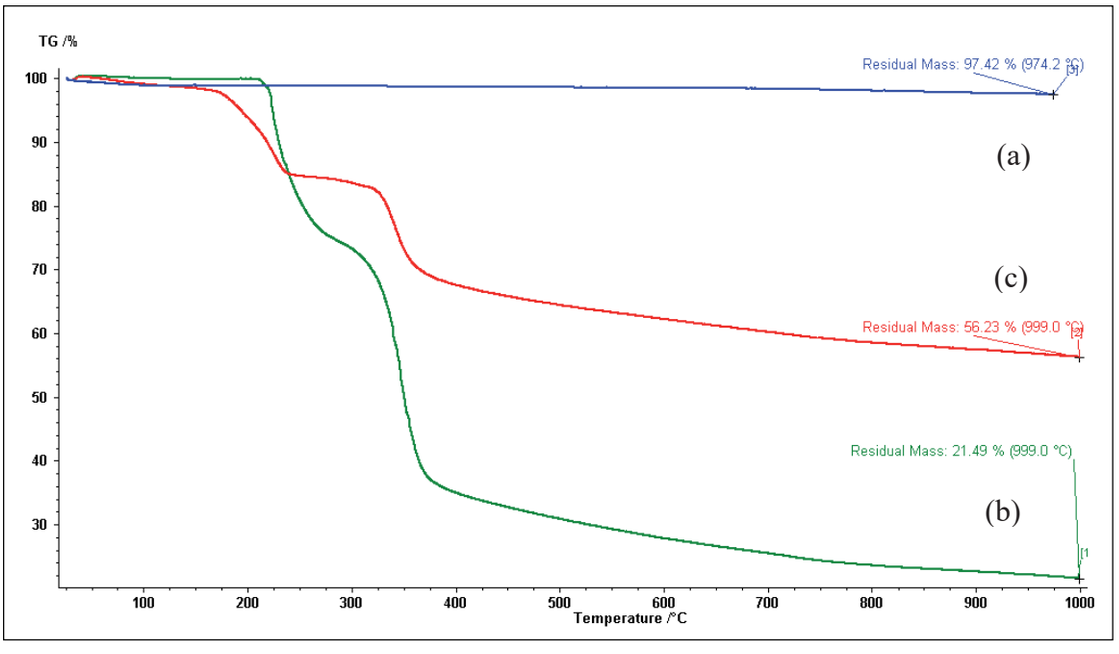


Fig. 1: TGA of glimepiride into mesoporous carrier SBA-15 (a) SBA-15 (b) Glimepiride (c) drug loaded carrier.

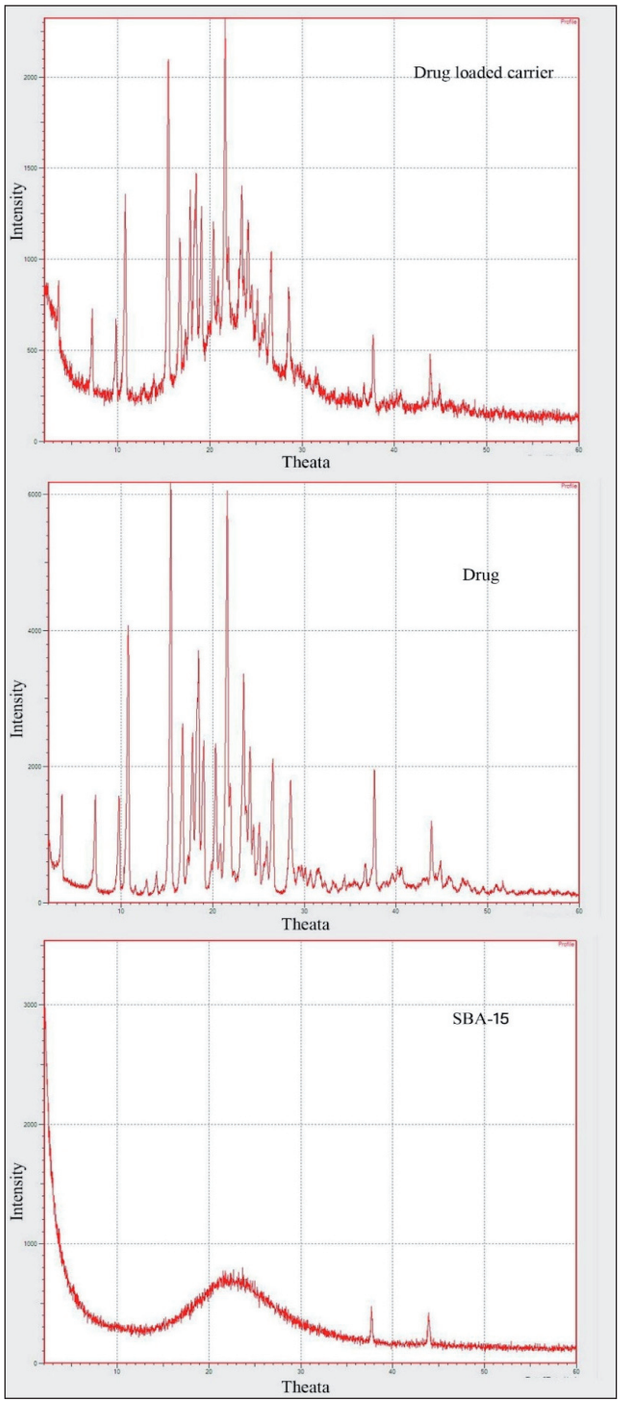


Fig. 2: XRD spectra of the (a) mesoporous SBA-15 (b) Glimepiride (c) Drug loaded carrier.

From these observations, it can be inferred that the crystalline nature of the drug was still maintained, but the relative reduction of diffraction intensity of glimepiride in carrier preparation at these angles suggests that the quality of the crystals was reduced (Valizadeh et al 2004). It shows the highest peak at 2θ of 1.9 degrees and low-intensity peaks at 2θ of 2.6 and 2.8 degrees. The pattern is in good agreement with previous literature data (Schmidt et al. 1995). PXRD pattern of glimepiride shows intrinsic peaks at 5.1, 11.6, 15.8, 18.6, and 26.2 ± 0.2 degrees at 2θ. They indicated the crystallinity of glimepiride. Analysis of glimepiride loaded SBA-15 spectrum confirmed glimepiride loading with distinctive peak appearance at 2θ of 26. This is an indication of glimepiride crystallization in the pores of the carriers. However, the remarkable weakened crystalline distinctive peaks of glimepiride indicated a less ordered crystallinity, rather than a completely amorphous state. It indicated a decrease in crystallinity and transformation into an amorphous state. Previous studies showed that higher drug loadings above 30% (w/w) could lead to incomplete amorphization, i.e., a small amount of crystalline drug could remain on the exterior surface of the generated particles. Drug molecules can theoretically be adsorbed onto the silica surface of mesopores as a monolayer or multilayers, depending on the drug's molecular dimension, accessible surface area, and pore size (Xu et al. 2016).

### *2.3.3. Fourier transform infrared spectroscopy (FTIR)*

To explicate the interaction between SBA-15 and glimepiride, FTIR was recorded for the drug, SBA-15 and the loaded carrier as shown in Fig. 3. It shows distinctive characteristic bands of SBA-15, and they are consistent with reported data (Wu et al. 2010). The IR spectra of SBA-15 and glimepiride loaded carriers were compared with the standard spectrum of glimepiride. IR spectrum of glimepiride is characterized by the absorption of carbonyl (C=O) sulphonyl urea group at 1686.9 and 1648.9 $cm^{-1}$ (Chowdhury and Majumdar 2010). Also the NH group which is located at 3322.3 $cm^{-1}$ and 3248.5 $cm^{-1}$ from the IR spectrum of glimepiride shifted to 3322.1 cm-1 in glimepiride loading SBA-15. The sulphonyl group bands are located at 1332.0 cm-1 and 1157.3 $cm^{-1}$ in pure glimepiride. In drug loaded carrier, the asymmetric vibration band of (S=O) band was shifted from 1332.0 $cm^{-1}$ to 1331.1 $cm^{-1}$ with decreased frequencies. In drug loaded carrier, the symmetrically stretching vibration band of (S=O) was shifted from 1157.3 $cm^{-1}$ to 1153.8 $cm^{-1}$ with decreased frequencies. The shift in the peaks associated with the sulfonylurea group of the glimepiride indicates an increase in bond strength possibility due to stabilizing effect of the hydrogen atoms of the sulphonyl group (Winters et al. 1997). This might be due to the formation of a hydrogen bond between the hydrogen atom of the NH group of glimepiride and one of the ion pairs of oxygen atom in the SBA-15 (Datt et al. 2013).

### *2.3.5. Particle size measurement*

Results show that the average particle size of three samples was 2785± 908. Figure 4 part (a) shows particle size distribution by intensity while part (b) shows particle size distribution by volume and part (c) shows particle size distribution by number.

## *2.4. Compression profile*

The area under the curve representing work displayed upon compression at all compression loads between 100 and 500 kg for mesoporous silica and the loaded samples is shown in Fig. 5.
The loaded sample requires less energy (work) for compression. In other words, the loaded sample displayed lower displacement upon compression at each compression load. This means that the loaded sample is highly packed and the application of compression forces imparts reduced volume reduction when compared to the mesoporous silica itself.
The Heckel plot of the samples is shown in Fig. 6. Parameters of the Heckel plot (yield pressure and intercept A) considered from the straight-line portion of three successive points are illustrated in Table 1.

**Table 1: Heckel equation parameters**

| Sample | Slope | $P_y$ | Intercept(A) |
|---|---|---|---|
| **SBA-15** | 0.02376 | 42.08 | 0.3902 |
| **SBA-15-loaded particles** | 0.002153 | 464.54 | 0.50236 |

Table 1 shows that the yield pressure ($P_y$) of the loaded mesoporous silica is much higher than that of the unloaded mesoporous silica. This means that the sample when loaded with glimepiride becomes highly fragmented compared to the mesoporous silica

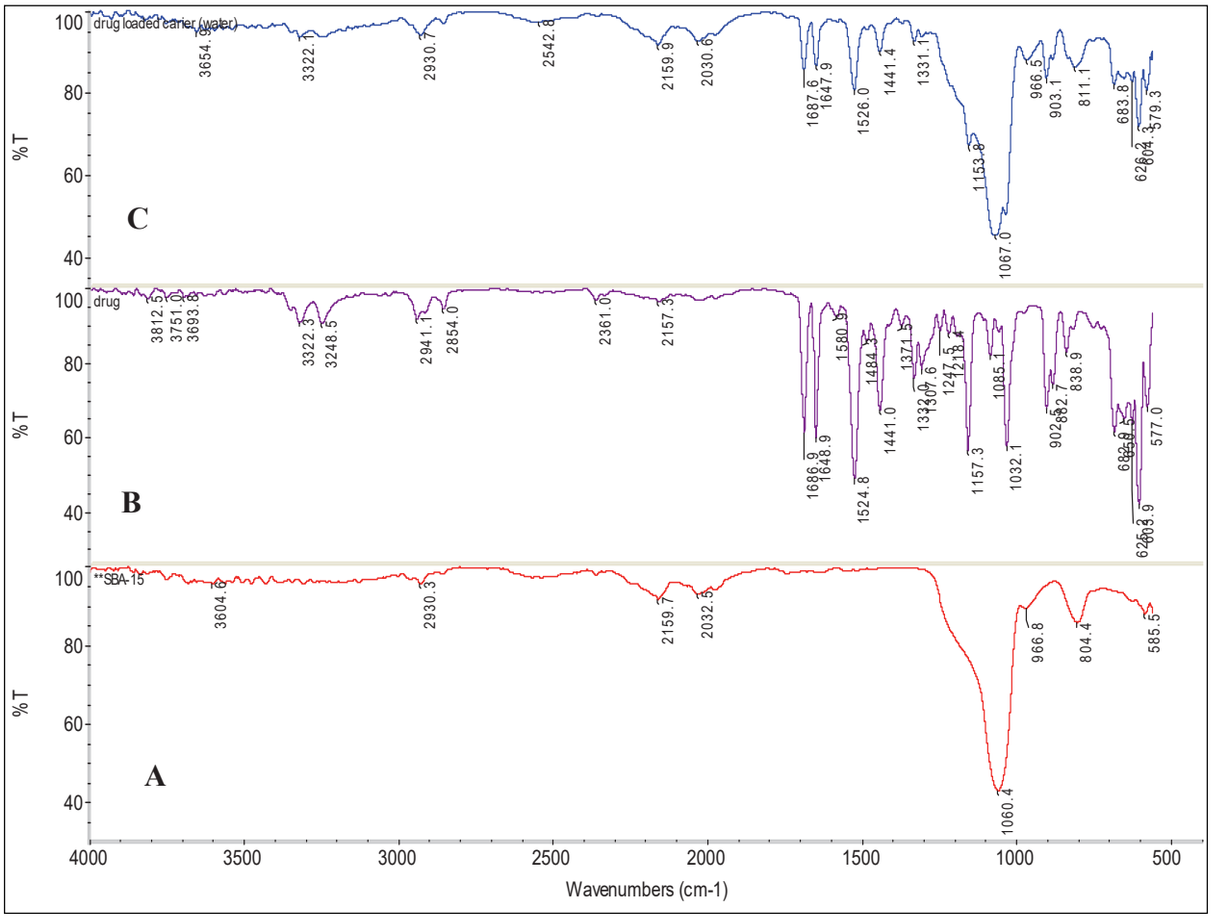


Fig. 3: Infrared spectra of (a) SBA-15, (b) Glimepiride and (c) Drug loaded carrier.

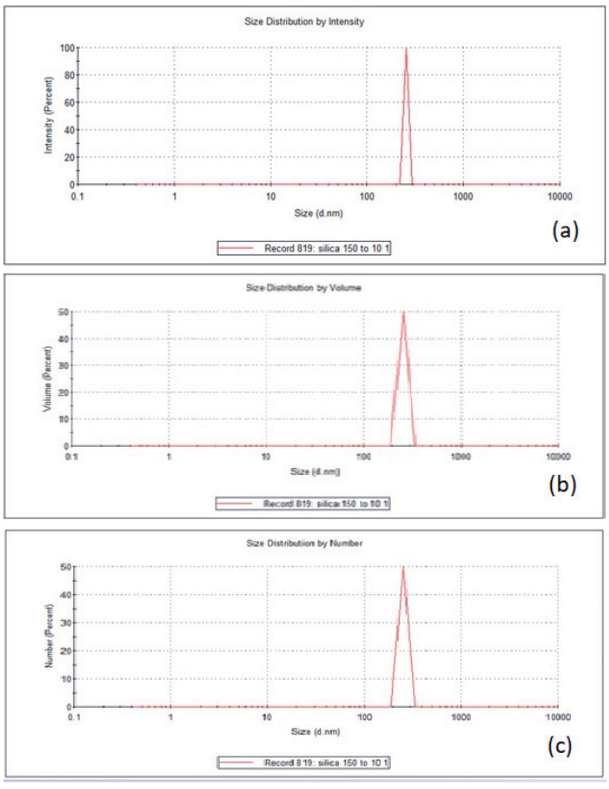


Fig. 4: Particle size measurement of one sample of loaded mesoporous silica (a) with glimepiride by intensity (b) with glimepiride by volume (c) with glimepiride by number.

itself. This is attributed to the fragmenting nature of the active material. Moreover, there is a high level of particle re-arrangement upon compression encountered by the loaded sample compared to the unloaded. Again, this high re-arrangement is normally a result of the high brittle-fracture nature of the loaded sample due to the presence of the API. High re-arrangement indicates an increased level of fragmentation of the loaded sample. Such high fragmentation tendency may explain the lower displacement of the loaded sample as the fragmenting pieces may have closed all the pores. Theoretically, the presence of these pores allows the movement of the particles when a force is applied. Kawakita analysis carried out for the polymer and loaded samples is presented in Fig. 7, parameters are further presented in Table 2.

**Table 2: Estimated Kawakita parameters**

| Sample | Slope | Intercept | A | Ab | B | 1/b |
|---|---|---|---|---|---|---|
| **SBA-15** | 1.1716 | 14.084 | 0.8535 | 0.0710 | 0.0831 | 12.021 |
| **SBA-15 loaded particles** | 1.2200 | 6.8989 | 0.81965 | 0.1449 | 0.1768 | 5.654 |

The "a" value for the mesoporous silica is higher than that for the loaded sample. This is expected as the "a" value indicates the extent of volume reduction with pressure. The mesoporous silica has higher volume reduction than the loaded sample. Such a result is concurrently aligned with the "ab" parameter which was higher for the loaded thus higher particle rearrangement. This is similar to the "A" value from the Heckel analysis. As the "1/b" parameter indicates the load needed to reduce the powder bed volume to half its initial value, the mesoporous silica itself needs a higher load for such reduction. In other words, there is more resistance to compression by the mesoporous silica compared to the loaded sample. Such resistance was eased when then glimepiride was

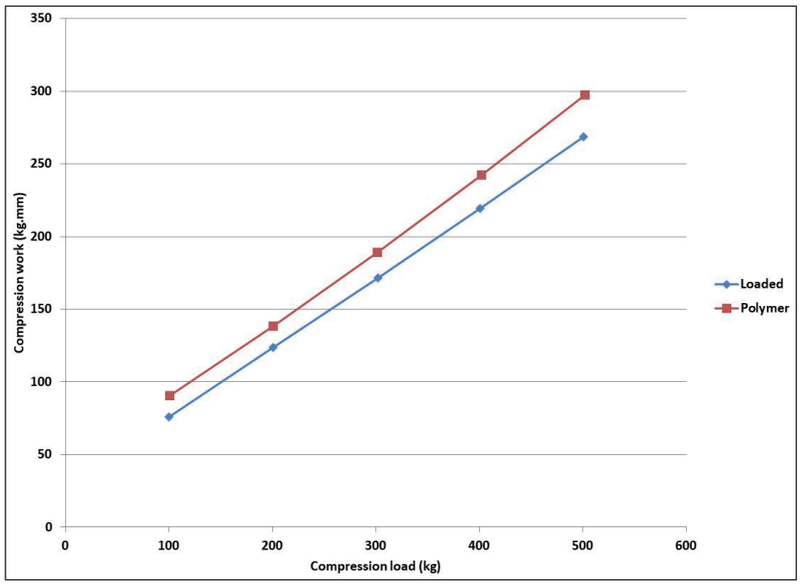


Fig. 5: The compression load versus compression work for the mesoporous silica and loaded mesoporous silica.

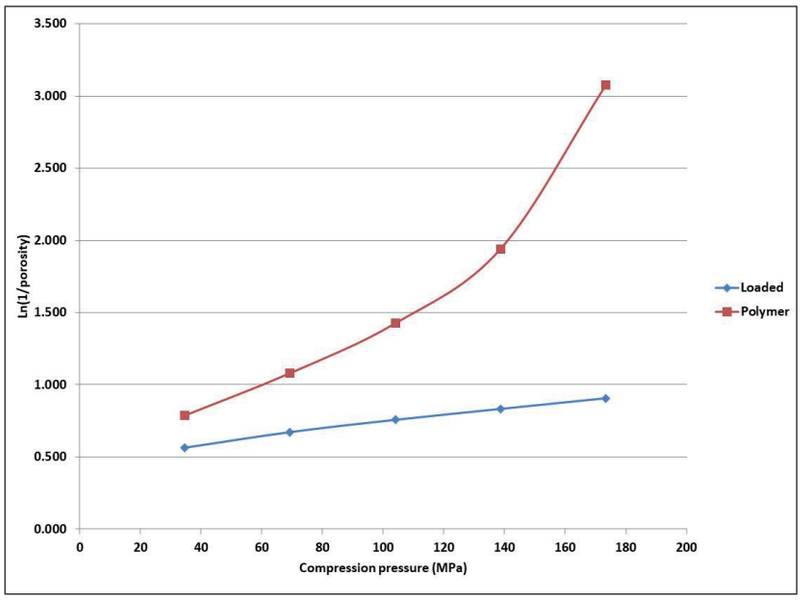


Fig. 6: Heckel plot of the mesoporous silica and loaded mesoporous silica.

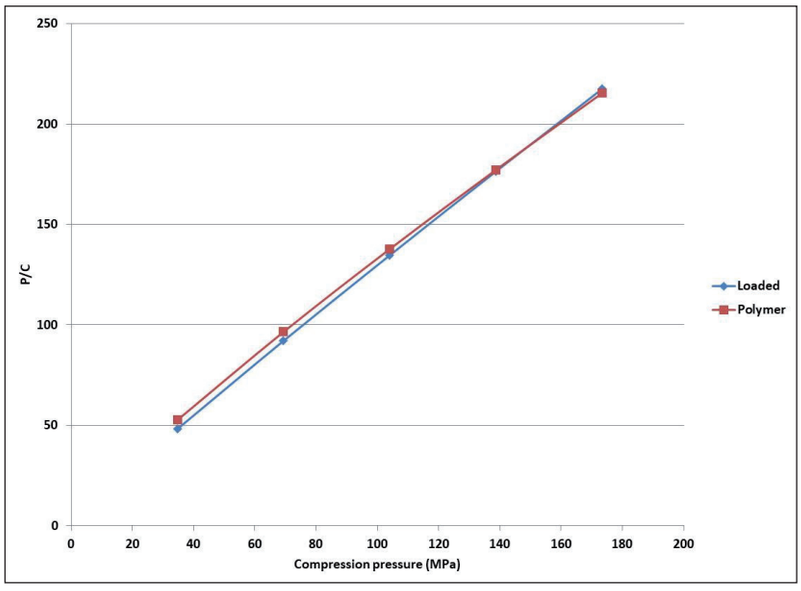


Fig. 7: Kawakita plot of loaded and unloaded mesoporous silica.

added in the loaded sample. This further indicates the high brittle-fracture nature of glimepiride.

### 2.5. In-vitro drug release study

Being a class II drug, glimepiride has poor aqueous solubility and slow dissolution rate. Consequently, the aim of this work was to improve the dissolution rate. An acidic dissolution medium (pH = 1) was selected as a discriminative media since glimepiride is a weak acidic drug. The dissolution profiles of pure glimepiride and glimepiride loaded in mesopause silica are presented in Fig. 8. The dissolution rate of glimepiride loaded mesoporous silica was significantly higher than that of the glimepiride raw material. Less than 10 % of the drug was released in 10 min in its raw form compared with about 70 % release from the mesoporous silica loaded mixture. This result indicated that mesoporous silica significantly improved the dissolution rate of glimepiride probably because of the large surface area on which the drug was adsorbed on it which gave positive impact on dissolution rate. The remaining 30 % of drug were released in approximately linear pattern. This may be the drug imbedded within the silica spheres and may be used later to provide controlled release of the drug.

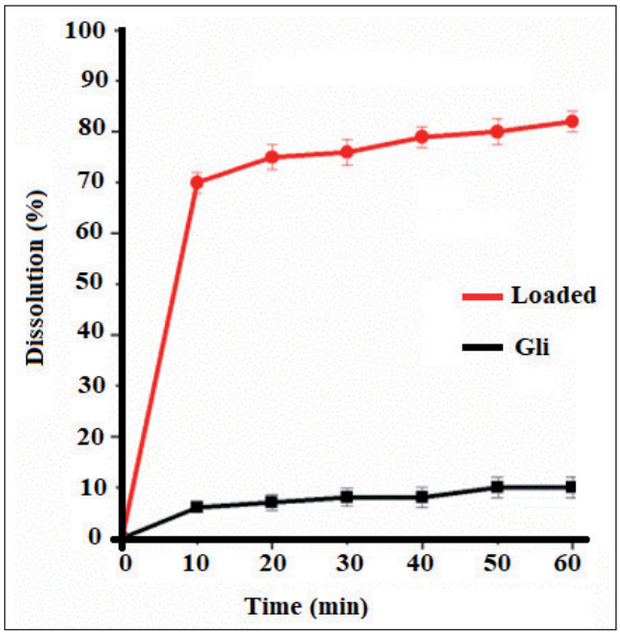


Fig. 8: dissolution rate profile of glimepiride powder and SBA-15 loaded glimepiride mesospheres.

### 2.6. Conclusions

SBA-15 was successfully synthesized and loaded with glimepiride, a slightly soluble drug, and characterized for its physical characteristics and drug loading. Maximum drug loading achieved by solvent method used was 40% and the prepared mesospheres were found to have improved compression properties and increase highly the dissolution rate of the model drug.

## 3. Experimental

### 3.1. Materials

Triblock copolymer (PEO20PPO70PEO20) was purchased from Acros Organics, New Jersey, US. Tetraethylorthosilicate (TEOS) was purchased from Aldrich, St. Louis-US. Glimepiride was kindly supplied by Pharma International, Jordan. Sodium hydroxide pellets (BDH, City Road, London), hydrochloric acid 35% (SD Fine-Chem Limited, Mumbai-India), and absolute ethanol 99.8% (AZ Chem, Pretoria-South Africa) were used as received. Hydrochloric acid 95% (Merck, New Jersey-US) was used to clean all glass equipment before use.

### 3.2. Synthesis of mesoporous silicate carrier SBA-15

SBA-15 was synthesized according to Zhao et al. (1998) with some changes. A solution of 2 M HCl (120 mL) was added to 30 mL deionized water. To the solution, 4.0 g of the triblock copolymer poly (ethylene oxide)-poly (propylene oxide)-poly (ethylene oxide) copolymers (PEO20PPO70PEO20) was added with continued stirring at 35 °C in a water bath until complete dissolution. Then, tetraethyl orthosilicate (TEOS; 8.5 g) was added dropwise under vigorous stirring until the polymer was completely dissolved. The obtained solution was left with stirring for 20 h. The mixture was aged in a teflon-coated stainless autoclave at 100 °C for 24 h. The obtained solid precipitate was filtered by suction filtration, washed with deionized water (3×50 mL) and dried at room temperature. The solid product was calcined at 550 °C for 8 h in a muffle furnace to remove the polymer template, thus producing the mesoporous silicate material SBA-15

### 3.3. Characterization of the prepared mesospheres

#### 3.3.1. Thermal gravimetric analysis (TGA)

Thermogravimetric analysis of the glimepiride, mesoporous SBA-15 and drug-loaded carrier was conducted in a NETZSCH STA 409 PC instrument (NETZSCH, Germany) using $N_2$ gas purge flow of 20 mL/min and a scan rate of 20 °C/min. For each run, a sample (10 mg) was placed into a hermetically sealed aluminum pan containing a pinhole. The sample cell was equilibrated at 25 °C and then heated to 1000 °C. Indium metal was used as the calibration standard.

#### 3.3.2. Powder X-ray diffraction (PXRD)

PXRD data for the glimepiride, mesoporous SBA-15 and drug-loaded carrier were collected using an XRD-7000 Shimadzu diffractometer (Japan), operating in transmission geometry with Cu-Kα radiation (λ = 1.5406 Å), 40 kV/100 mA. The samples were prepared on silicon single crystal sample holders with a 20 mm depth. Data for each sample were collected from 2θ = 5° to 50° at 25 °C with a step and scan rate of 2°/min.

#### 3.3.3. Fourier transfer infra-red (FT-IR)

Each sample of glimepiride, SBA-15, and drug-loaded carrier (1 mg) was ground into a powder with dried KBr (50 mg) in a mortar and the mixture was pressed into a piece of slice and the FT-IR spectra were recorded using a Thermo Nicolet NEXUS 670 FT-IR spectrometer in the range of 4000–400 $cm^{-1}$.

#### 3.3.4. Scanning electron microscopy (SEM)

The morphologies of the prepared SBA-15 solid samples were characterized by scanning electron microscopy (SEM) using a FEI-FEG INSPEC F50 instrument. Photos were taken for particle size measurement of the prepared mesospheres and to the loaded ones.

#### 3.3.5 Particle size measurement

Particle size distribution and polydispersity index were measured by photon correlation spectroscopy (PCS) using the dynamic light scattering (DLS) Zetasizer Nano ZS (Malvern, Worcestershire, UK). Silica particles sample of 10 mg were suspended in 10 ml deionized water. After that particles were re-dispersed using an ultra-prob sonicater for 3 min. Prior the measurement, the suspension was diluted 125-fold using deionized water. The refractive index values for silica and water are 1.48 and 1.333, respectively. Observation was done in three measurements with three runs each.

### 3.4. Drug loading on SBA-15 particles

The loading process of guest molecules on the mesoporous silica is based on physical adsorption process. Glimepiride was loaded into samples of mesoporous SBA-15 by the following general procedure: glimepiride (0.200 g) was suspended in water (25.0 mL) and then added to a flask containing mesoporous SBA-15 (0.200 g). The mixture was stirred in the dark, at ambient temperature, for 24 h. The solid of the drug-loaded carrier was filtered and dried under vacuum (30 mmHg) for 2 h at 60 °C.

### 3.5. Drug assay

The concentration of glimepiride was determined using ultraviolet-visible spectrophotometry at a wavelength of 250 nm. The linearity of the ultraviolet-visible spectrophotometry method was investigated by measuring the absorbance of the working standard solutions at 250 nm. They were prepared immediately before use by suitable dilutions of the 500 µg/mL stock solution to appropriate concentration levels (5, 10, 20, 30, 40, 50 µg/mL) by diluting (0.05, 0.1, 0.2, 0.3, 0.4, 0.5 mL) of the stock solution up to 10 mL using volumetric flask in distilled water. A calibration curve was constructed by plotting the absorbance of the working standard solutions of the drug as a function of the concentration and the regression equations were calculated.

### 3.6. Determination of drug loading

The drug-loaded capacity was determined by the ultraviolet-visible spectrophotometric method. A weight of 10 mg of glimepiride loaded SBA-15 (1:1 ratio) was placed in a 100 mL volumetric flask, that was filled up to volume with distilled water. The contents were stirred with a magnetic stirrer for 24 h at room temperature. After

this period, the supernatant was filtered through a 0.45 µm PTFE syringe filter. The concentration of the solubilized glimepiride in the clear filtrate was determined using Beer-Lambert law. The concentration was determined at a wavelength of 250 nm after suitable dilution with distilled water. The concentration of the solubilized glimepiride in the clear filtrate was determined using the linear equation of the Beer-Lambert law of glimepiride of the standard calibration curve ($y = 0.01674 x - 0.03262$; $R^2 = 0.999$) in the phosphate buffer of pH 6.8 over the range of (5-50) µg/mL. Percentage of drug loading Eq. (3) after multiplying the concentration with the appropriate dilution factor and the final volume was calculated as followed:

$$\%\ Drug\ Loading = \frac{Mass\ of\ loaded\ \text{Glimepiride}}{Mass\ of\ MCM-48} \times 100\% \quad (3)$$

### *3.7. Analysis of compression output and energy consumption of powdered particles*

For this study, a Gamlen Tablet Press, GTP (Gamlen Tableting Ltd. Biocity Nottingham, UK) was used. Upon compression, the GTP-1 controller tracks the upper punch displacement (mm) in relation to the applied load (kg) and generates load-displacement curves. The resulted data is used to calculate the work of compression (W) represented by the area under the compression curve.

The in-die compressibility properties of the powders were determined using Heckel and Kawakita equations. The Heckel equation (Eq. 4) measures the change in porosity reduction of powders when subjected to compression pressure *P* (MPa) :

$$ln\frac{1}{porosity} = kP + A \quad (4)$$

where *k* is the slope of the linear portion of the curve that is used to calculate the yield pressure (*Py*) which is the inverse of *k*. $P_y$ (MPa) is a measurement of the plasticity or brittle-fracture of the material. The lower the *PY* value the higher the plasticity the material undergoes upon compression. The parameter *A* is related to the die filling and rearrangement of particles.

Kawakita analysis (Eq. 5) is used to correlate compressibility with the degree of volume reduction, *C*, of powders when subjected to compression pressure, *P* (MPa :

$$\frac{P}{C} = \frac{P}{a} + \frac{1}{ab} \quad (5)$$

where "*a*" is a constant related to the porosity of the material, whereas the constant *b* relates to the plasticity of the material and *ab* is a constant that indicates the degree of particles rearrangement within the die. The reciprocal of *b* (*1/b*) represents the pressure required to reduce the bulk volume of the powder tested by 50%.

### *3.7. In-vitro drug release*

The dissolution rate of pure glimepiride (50 mg) and glimepiride loaded powder (equivalent to 50 mg) were studied by using a U.S. pharmacopoeia tablet dissolution test apparatus at a paddle rotation speed of 100 rpm in 900 mL of 0.1 N HCl containing 0.25% (w/v) of sodium lauryl sulfate as a dissolution medium at 37.5 ± 0.5 °C. At specified times, 5 mL samples were withdrawn by a syringe with a nylon 0.45 µm filter (Titan, Shanghai, China). Withdrawn samples were replaced with a fresh medium that was pre-warmed to 37 °C. The content of glimepiride was calculated from a prepared calibration curve measured at 273 nm using a UV-Visible spectrophotometer (Shimadzu UV2600, Shimadzu, Japan). Dissolution rates were performed in triplicate.

Acknowledgments: The authors would like to thank PDRC in Al-Ahliyya Amman University for supporting this work especially, the Dean of Faculty of Pharmacy and Director of PDRC Prof. M. El-Tanani. Thanks are extended to all the colleagues and assistants who made contribution in this work in University of Petra and University of Jordan.

Conflicts of interest: None declared.

## References

Abbaspour S, Nourbakhsh AA, Kalbasi RJ, Mackenzie KJ (2012) Investigating the properties of the nanocomposite (poly(4-vinyl pyridine)/Al-SBA-15): a precursor for β-SiAlON. Mol Cryst Liq Cryst 555: 104–111.

Abdelhamid S (2000) Novel synthesis of high-quality MCM-48 silica. J Am Chem 122: 6504–6505.

Amidon GL, Lennernas H, Shah VP, Crison JR (1995) A theoretical basis for a biopharmaceutic drug classification: the correlation of in vitro drug product dissolution and in vivo bioavailability. Pharm Res 12: 413–420.

Attia AK, Ibrahim MM. El-Ries MAN (2013) Thermal analysis of some antidiabetic pharmaceutical compounds. Adv Pharm Bull 3: 419–424.

Balas F, Manzano M, Horcajada P, Vallet-Regı M (2006) Confinement and controlled release of bisphosphonates on ordered mesoporous silica-based materials. J Am Chem 128: 8116–8117.

Bala S, Kataria MK, Bilandi A (2014) An overview on solid dispersion techniques implemented for dissolution anhancement of glimepiride. Am J Pharmtech Res 4 (4): 65–77.

Bhattacharyya SG, Lelong G, Saboungi, ML. (2006) Recent progress in the synthesis and selected applications of MCM-41: J Exp Nanosci 1: 375–395.

Chaudhari MD, Sonawane RO, Zawar L (2012) Solubility and dissolution enhancement of poorly water soluble glimepiride by using solid dispersion technique. Int J Pharm Pharm Sci 4: 534–539.

Chowdhury S, Majumdar S (2010) Statistical optimization of fixed dose combination of glimepiride and atorvastatin calcium mediate release tablet formulation. Int J Pharm Pharm Sci 2 (Suppl. 4): 194–200.

da Silva LCC, dos Reis TVS, Cosentino IC, Fantini MCA, Matos JR. Bruns RE (2010) Factorial design to optimize microwave-assisted synthesis of FDU-1 silica with a new triblock copolymer. Micropor Mesopor Mater 133: 1–9.

Datt A, Burns EA, Dhuna NA, Larsen SC. Loading and release of 5-fluorouracil from HY (2013) zeolites with varying SiO2/Al2O3 ratios Micropor Mesopor Mater 167: 182–187.

Doadrio AD, Sousa EM, Doadrio JC, Pérez-Pariente P, Barba II, Vallet MR (2004) Mesoporous SBA-15 HPLC evaluation for controlled gentamicin drug delivery. J Control Release 97: 125–132.

Doadrio JC, Edesia MB, Barba II, Doadrio AL, Pérez-Pariente J, Vallet MR (2006) Functionalization of mesoporous materials with long alkyl chains as a strategy for controlling drug delivery. J Mater Chem 16: 462–466.

Doadrio A, Doadrio JC, Sánchez-Montero JM, Salinas AS, Vallet MR (2010). A rational explanation of the vancomycin release from SBA-15 and its derivative by molecular modeling. Micropor Mesopor Mater 132: 559–566.

Fagundes L, Sousa TG, Sousa A, Silva AA, Sousa EM (2006). SBA-15-Collagen hybrid material for drug delivery applications. J Non Crystal Solids 352: 3496–3501.

Fruijtier-Pölloth C (2012) The toxicological mode of action and the safety of synthetic amorphous silica-a nanostructured material. Toxicol 294: 61–79.

Han YJ, Stucky GD, Butler A (1999) Mesoporous silicate sequestration and release of proteins. J Am Chem Soc 42: 9897–9898.

Huang MH, Choudrey A, Yang P (2000) Ag nanowire formation within mesoporous silica. Chem Commun 2000: 1063–1064.

Izquierdo-Barba I, Doadrio JS, Doadrio, AL, Pérez Pariente J, Martinez A, Babonneau F, Vallet-Regi M (2009) Influence of mesoporous structure type on the controlled delivery of drugs: release of ibuprofen from MCM-48, SBA-15 and functionalized SBA-15. J. Sol Gel Sci Tech 50: 421–429.

Le TT, Elyafi AK, Mohammed, A, Al-Khatwani A (2019) Delivery of poorly soluble drugs via mesoporous silica: impact of drug overloading on release and thermal profiles. Pharmaceutics 11: 269–285.

Liu AM, Hidajat K, Kawi S, Zhao DY (2000) A new class of hybrid mesoporous materials with functionalized organic monolayers for selective adsorption of heavy metal ions. Chem Commun 13: 1145–1146.

Massi-Benedetti M (2003). Glimepiride in type 2 diabetes mellitus: a review of the worldwide therapeutic experience. Clin Ther 25: 799–816.

Malhis AA, Arar HS, Fayyad KM, Hodali AH (2018) Amino- and thiol-modified microporous silicalite-1 and mesoporous MCM-48 materials as potential effective adsorbents for Pb(II) in polluted aquatic systems. Adsorp SciTechnol 36: 1-2.

Mellaert R, Fayad EJ, Van den Mooter G, Augustijns P, Rivallan M, Thibault-Starzyk F, Martens JA (2013) In situ FT-IR investigation of etravirine speciation in pores of SBA-15 ordered mesoporous silica material upon contact with water. Mol Pharm 10: 567–573.

Mokale VJ, Naik JB, Verma U, Patil JS, Yadava SK (2014) Preparation and characterization of biodegradable glimepiride loaded PLA nanoparticles by o/w solvent evaporation method using high pressure homogenizer: a factorial design approach, SAJ Pharm Pharmacol 1: 2375–2262.

Qu f, Zhu G, Huang S, li S, Sun J, Zhang D, Qui S (2006) Controlled release of Captopril by regulating the pore size and morphology of ordered mesoporous silica. Micropor Mesopor Mater 92: 1–9.

Rani RS, Lohita M, Preethi PJ, Madhavi R, Sunisitha B, Mounika D (2014) Glimepiride. A review of analytical methods. Asian J Pharm Anal 4: 178–182.

Rosenholm J, Lindén M (2008) Towards establishing structure–activity relationships for mesoporous silica in drug delivery applications. J Control Release 128: 157–164.

Schmidt R, Stucker S, Akporiaye D (1995) High-resolution electron microscopy and X-ray diffraction studies of MCM-48. Micropor Mater 5: 1–7.

Schumacher K, Grun M, Unger K (1999) Novel synthesis of spherical MCM-48. Micropor Mesopor Mater 27: 201– 206.

Singh OB, Biswal S, Sahoo J, Murth PN (2009) Physicochemical properties of glimepiride in solid dispersions with polyethylene glycol 20000. Int J Pharm Sci Nanotech 2: 537–543.

Tiwari A, Mishra MK, Nayak K, Verma G, Yadav SK, Shukla N (2016)
A review article on glimeperide: an oral hypoglycaemic drug. Int J Adv Res 4: 920–927.

Vallet-Regi M, Rámila A, del Real RP, Pérez-Pariente J (2001) A new property of MCM-41: drug delivery system. Chem Mater 13: 308–311.

Vallet-Regi M, Doadrio JC, Doadrio AI, Zquierdo-Barba I, Pérez-Pariente J (2004), Hexagonal ordered mesoporous material as a matrix for the controlled release of amoxicillin. Solid State Ionics 172: 435–439.

Vallet-Regi M, Balas F, Arcos D (2007) Mesoporous materials for drug delivery. Angew Chem Int Ed 46: 7548–7558.

Valizadeh H, Nokhodchi A, Qarakhani N, Zakeri-Milani P, Azarmi S, Hassanzadeh D Löbenberg R(2004) Physicochemical characterization of solid dispersions of indomethacin with PEG 6000, Myrj 52, lactose, sorbitol, dextrin, and Eudragit® E100. Drug Devel Ind Pharm 30: 303–317.

Wagh VT, Jagtap VA, Shaikh TJ, Nandedkar SY (2012). Formulation and evaluation of glimepiride solid dispersion tablets for their solubility enhancement. J Adv Sci Res 3: 36–41.

Winters S, York P, Timmins P (1997) Solid state examination of a gliclazide: beta-cyclodextrin complex. Eur J Pharm Sci 5: 209–214.

Wu S, Li F, Xu R(2010) Synthesis of thiol-functionalized MCM-41 mesoporous silicas and its application in Cu(II), Pb(II), Ag(I), and Cr(III) removal. J Nanopart Res12: 2111–2124.

Xu WJ, Xie HJ, Cao QR, Shi LL, Cao Y, Zhu XY, Cui JH (2016) Enhanced dissolution and oral bioavailability of valsartan solid dispersions prepared by a freeze drying technique using hydrophilic polymers. Drug Deliv 23: 41–48.

Yu H, Zhai QZ (2009) Mesoporous SBA-15 molecular sieve as a carrier for controlled release of nimodipine. Micropor Mesopor Mater 123: 298–305.

Zhao DY, Feng JL, Huo QS, Feng JL, Chmelka, BF, Stucky GD (1998) Nonionic triblock and star diblock copolymer and oligomeric surfactant syntheses of highly ordered, hydrothermally stable, mesoporous silica structures. J Am Chem Soc 120: 6024–6036.

Zhang L, Yang M, Li Y, Guo R, Jiang X, Yang C, Liu B (2007), 10-Hydroxycamptothecin loaded nanoparticles: Preparation and antitumor activity in mice. J Control Release 119: 153–162.

Zhao P, Liu MC, Lin HC, Yarat A (2017) Synthesis and drug delivery applications for mesoporous silica nanoparticles. J Med Biotechnol 1: 1–8.

Ziarani GM, Badiei A, Haddadpour M (2011) Application of sulfonic acid functionalized nanoporous silica (SBA-Pr-SO3H) for one-pot synthesis of quinoxaline derivatives. Int J Chem 3: 87–94.